Role of Spin Noise in the Detection of Nanoscale Ensembles of Nuclear Spins

C. L. Degen,[1] M. Poggio,[1,2] H. J. Mamin,[1] and D. Rugar[1,*]

[1]IBM Research Division, Almaden Research Center, 650 Harry Road, San Jose, California 95120, USA
[2]Center for Probing the Nanoscale, Stanford University, 476 Lomita Hall, Stanford, California 94305, USA

(Received 11 October 2007; published 20 December 2007)

When probing nuclear spins in materials on the nanometer scale, random fluctuations of the spin polarization will exceed the mean Boltzmann polarization for sample volumes below about $(100\ \mathrm{nm})^3$. In this Letter, we use magnetic resonance force microscopy to observe nuclear spin fluctuations in real time. We show how reproducible measurements of the polarization variance can be obtained by controlling the spin correlation time and rapidly sampling a large number of independent spin configurations. This allows significant improvement in the signal-to-noise ratio for nanometer-scale magnetic resonance imaging.

DOI: 10.1103/PhysRevLett.99.250601 PACS numbers: 05.40.−a, 07.55.−w, 76.60.−k

Magnetic resonance signals detected in conventional magnetic resonance imaging (MRI) experiments originate from the slight alignment of nuclear spins induced by an external magnetic field. This thermal equilibrium (''Boltzmann'') polarization gives rise to a mean fractional spin polarization that is typically quite small, $\overline{\Delta N}/N < 10^{-4}$. For the large ensembles of nuclear spins detected in MRI experiments, usually $N > 10^{15}$ spins, the Boltzmann polarization is the dominant source of spin alignment. However, as new techniques, such as magnetic resonance force microscopy (MRFM) [1,2], push detectable volumes below $(100\ \mathrm{nm})^3$, another type of polarization becomes increasingly important: the ''statistical'' polarization.

Statistical polarization arises from the incomplete cancellation of randomly oriented spins. The instantaneous polarization, i.e., the difference ΔN between spin-up and spin-down populations, can be either positive or negative and will fluctuate on a time scale that depends on the random flip rate of the spins (for example, due to spin-lattice relaxation). For a random ensemble of spin-1/2 nuclei, it follows from the properties of the binomial distribution that the statistical fluctuations have variance $\sigma^2_{\Delta N} = N[1 - (\overline{\Delta N}/N)^2]$, where the overbar indicates mean value. In the limit of small mean polarization, which is representative of most experiments, the variance simplifies to $\sigma^2_{\Delta N} = N$. The existence of statistical polarization was pointed out by Bloch in his seminal paper on nuclear induction [3] and has been observed experimentally by a number of techniques, including superconducting quantum interference devices [4], conventional magnetic resonance detection [5–7], optical techniques [8], and MRFM [2,9].

As detection volumes enter the nanometer-scale regime, the standard deviation of the polarization fluctuations $\sigma_{\Delta N}$ can easily exceed the Boltzmann polarization $\overline{\Delta N} = N\mu B/k_B T$, where μ is the magnetic moment of the spin, B is the polarizing magnetic field, and T is the temperature [10]. The dominance of statistical polarization, as defined by $\sigma_{\Delta N} > \overline{\Delta N}$, occurs for sample volumes $V < (\mu B/k_B T)^{-2}\rho_N^{-1}$, where $\rho_N = N/V$ is the spin number density. Assuming conditions representative of high-field MRI microscopy of protons in water ($B = 10$ T, $T = 295$ K, and $\rho_N = 7 \times 10^{28}\ \mathrm{m}^{-3}$), the volume corresponds to $\sim(230\ \mathrm{nm})^3$. For MRFM detection of ^{19}F nuclei in calcium fluoride, as considered in this Letter ($B = 2.9$ T, $T = 4.5$ K and $\rho_N = 5 \times 10^{28}\ \mathrm{m}^{-3}$), the volume for statistical polarization dominance is $\sim(37\ \mathrm{nm})^3$.

Given that statistical polarization is such a strong feature of nanoscale nuclear spin detection, it is worthwhile to consider efficient methods to harness it for imaging applications. In order to generate a signal that is proportional to the spin density, it is natural to consider using the variance as the ''signal.'' If the polarization ΔN is measured for n independent configurations of the spin ensemble, the sample variance $s^2_{\Delta N}$ is estimated as

$$s^2_{\Delta N} = \frac{1}{n-1}\sum_{j=1}^{n}(\Delta N_j - \overline{\Delta N})^2. \tag{1}$$

(The symbol σ^2 is used to denote the true or theoretical variance, while s^2 is the estimated or ''sample'' variance.)

The variance estimate $s^2_{\Delta N}$ is subject to some uncertainty since only a limited number of independent spin configurations can be sampled. Textbooks on statistics, e.g., Ref. [11], show that the standard error of $s^2_{\Delta N}$ is

$$\sigma_{s^2_{\Delta N}} = \left(\frac{2}{n-1}\right)^{1/2}\sigma^2_{\Delta N} \approx \left(\frac{2}{n-1}\right)^{1/2} N. \tag{2}$$

If this ''spin noise'' is the only noise present, the overall signal-to-noise ratio (SNR) for the variance determination depends only on n,

$$\mathrm{SNR} \equiv \frac{\sigma^2_{\Delta N}}{\sigma_{s^2_{\Delta N}}} = \left(\frac{n-1}{2}\right)^{1/2}. \tag{3}$$

This equation reveals a basic strategy for statistical spin detection: one should rapidly sample as many independent spin configurations as possible. Independent spin configurations can be obtained by periodically rerandomizing the ensemble.

The above analysis of the SNR represents an idealized case. In real experiments, the spin polarization is measured via an intermediate quantity, such as the magnetic force, and the measurements are corrupted by noise. In our experiments, the measurement noise, including the cantilever thermal noise, is significant, and the spin signals have a finite correlation time. These factors must be taken into account when analyzing the signal statistics.

As shown in Fig. 1, we observe the nuclear spin polarization using an ultrasensitive cantilever to detect the attonewton magnetic force between spins in the sample and a nearby magnetic tip [1,12]. The cantilever mechanical resonance is driven by cyclic adiabatic spin inversions induced by rf frequency sweeps, and by thermal noise. A fiber-optic interferometer monitors the resulting cantilever motion and the cantilever oscillation signal is synchronously detected by a two-channel lock-in amplifier. The phase of the lock-in amplifier is set so that the spin signal plus thermal noise appear in the in-phase (X) channel, while only thermal noise is present in the quadrature (Y) channel. The lock-in signals are digitized and low-pass filtered in software so as to control the overall measurement bandwidth. Since the spin signal and the measurement noise are statistically independent, the variance of the

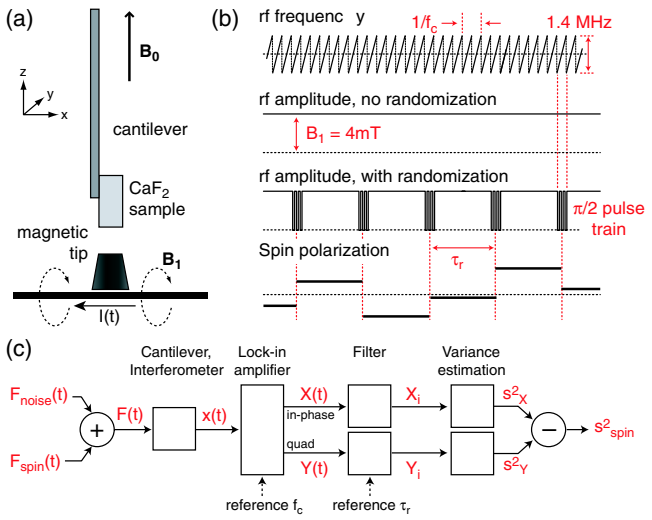

FIG. 1 (color online). (a) Experimental setup. A (4 μm)^3 CaF_2 particle attached to the end of a single-crystal Si cantilever (f_c = 2.6 kHz, k_c = 86 μN/m, and Q = 18 500) is positioned 80 nm above a FeCo-magnetic tip and placed in a static external field B_0 = 2.85 T ($B_0||\mathbf{z}$). ^{19}F spins are excited by an rf magnetic field B_1 = 4 mT ($B_1||\mathbf{y}$), generated by passing current $I(t)$ through a microwire situated directly under the tip [16]. All experiments are carried out at 4.2 K and in high vacuum. (b) Protocol used for spin detection and randomization. Repetitive rf frequency sweeps with a center frequency of 114.8 MHz invert the spins adiabatically twice per cantilever cycle [17,18]. For spin randomization, the rf field is interrupted at fixed intervals τ_r by a burst of $\pi/2$ pulses. Spin polarization is completely uncorrelated before and after randomization pulses. (c) Signal processing protocol as described in the text.

in-phase channel is given by $\sigma_X^2 = \sigma_{\text{spin}}^2 + \sigma_{\text{noise}}^2$. The quadrature channel measures only noise, so $\sigma_Y^2 = \sigma_{\text{noise}}^2$. The spin portion of the variance is then given by $\sigma_{\text{spin}}^2 = \sigma_X^2 - \sigma_Y^2$.

In the experiment, the in-phase and quadrature channels are recorded for a time τ_{total} and the spin signal variance s_{spin}^2 is estimated from the measured sample variances according to $s_{\text{spin}}^2 = s_X^2 - s_Y^2$. We now seek an expression for the SNR associated with s_{spin}^2 that is similar to Eq. (3), but also includes measurement noise. To obtain statistically independent spin configurations, the spins are periodically randomized at intervals separated by time τ_r using a burst of $(\pi/2)$ rf pulses. The spin polarization remains essentially constant between randomizations if $\tau_r \ll \tau_m$, where τ_m is the correlation time of the naturally fluctuating spin polarization [13]. In order to keep the analysis simple we assume that the X and Y channels are filtered using convolution-type filters that average the signals in the intervals between the periodic randomizations. The actual experiment used first order low-pass filters instead of the assumed averaging filters, resulting in a slight reduction of SNR performance [14].

The output of the averaging filters is assumed to be sampled synchronously with the randomizations, resulting in the measurement sequences X_i and Y_i, where $i = 1, \ldots, n$ and $n = \tau_{\text{total}}/\tau_r$ are the number of independent spin configurations. From these samples, the variances s_X^2 and s_Y^2 are calculated as in Eq. (1). The associated standard errors are $\sigma_{s_X^2} = [2/(n-1)]^{1/2}\sigma_X^2$ and $\sigma_{s_Y^2} = [2/(n-1)]^{1/2}\sigma_Y^2$. The standard error of s_{spin}^2 is then given by $\sigma_{s_{\text{spin}}^2} = (\sigma_{s_X^2}^2 + \sigma_{s_Y^2}^2)^{1/2}$, or $\sigma_{s_{\text{spin}}^2} = \{\frac{2}{n-1}[(\sigma_{\text{spin}}^2 + \sigma_{\text{noise}}^2)^2 + (\sigma_{\text{noise}}^2)^2]\}^{1/2}$. The SNR can then be written as

$$\text{SNR} \equiv \frac{\sigma_{\text{spin}}^2}{\sigma_{s_{\text{spin}}^2}} = \left(\frac{\tau_{\text{total}}/\tau_r - 1}{2}\right)^{1/2}\left[1 + 2\frac{\sigma_{\text{noise}}^2}{\sigma_{\text{spin}}^2} + 2\frac{\sigma_{\text{noise}}^4}{\sigma_{\text{spin}}^4}\right]^{-1/2}. \quad (4)$$

Note that in the absence of measurement noise, (4) is consistent with the previous result in (3).

To finish the analysis, we need to know how σ_{noise}^2 depends on the randomization interval τ_r. For a convolution filter that averages the signal over the randomization interval τ_r, the power transfer function is $|G(f)|^2 = \sin^2(\pi f \tau_r)/\pi^2 f^2 \tau_r^2$, which has an equivalent noise bandwidth of $\Delta f = 1/2\tau_r$ (single-sided with units of Hz). The noise variance is given by $\sigma_{\text{noise}}^2 = S_{\text{noise}}\Delta f = S_{\text{noise}}/2\tau_r$, where S_{noise} is the single-sided power spectral density of the measurement noise in each channel. We assume this spectral density to be independent of frequency within the bandwidth of the filter. This is the case in our experiments, where the cantilever thermal noise has a relatively broad

spectrum since the cantilever is strongly damped by feedback. The SNR can thus be written as

$$\mathrm{SNR} = \left(\frac{\tau_{\mathrm{total}}/\tau_r - 1}{2}\right)^{1/2}\left[1 + \frac{S_{\mathrm{noise}}}{\tau_r \sigma^2_{\mathrm{spin}}} + \frac{S^2_{\mathrm{noise}}}{2\tau_r^2 \sigma^4_{\mathrm{spin}}}\right]^{-(1/2)}. \quad (5)$$

From the above equation, the SNR is found to be maximized when the randomization period is $\tau_r = S_{\mathrm{noise}}/\sqrt{2}\sigma^2_{\mathrm{spin}}$, which is equivalent to choosing a randomization rate and associated filter bandwidth such that $\sigma^2_{\mathrm{noise}} = \sigma^2_{\mathrm{spin}}/\sqrt{2}$. With this choice of τ_r and assuming that $\tau_{\mathrm{total}} \gg \tau_r$, we find

$$\mathrm{SNR}_{\mathrm{max}} = \left(\frac{\sigma^2_{\mathrm{spin}}\tau_{\mathrm{total}}}{2(\sqrt{2}+1)S_{\mathrm{noise}}}\right)^{1/2}. \quad (6)$$

We have experimentally demonstrated the advantage of periodic spin randomization while measuring statistical polarization of ^{19}F in a CaF_2 single-crystal sample. In Fig. 2(a) we show a typical 60 s duration record of $X(t)$ from the lock-in amplifier as the spins are cyclically inverted by rf frequency sweeps. This output contains contributions from both the spins and the thermal noise, while the quadrature channel signal $Y(t)$, shown in Fig. 2(b), is predominantly just thermal noise. The X channel variance is 0.32 Å^2, which corresponds to a force variance of approximately 450 aN^2. The Y channel variance is much smaller, about 0.055 Å^2, which corresponds to a thermal force variance of 78 aN^2. Based on an estimated lateral field gradient of 10^6 T/m, the observed spin fluctuations in the X channel correspond to an rms statistical polarization of about 1500 ^{19}F spins.

The spin fluctuations in Fig. 2(a) can be seen by inspection to have long correlation times, on the order of seconds. By calculating the autocorrelation function associated with this and other similar time records, the autocorrelation was found to be well fit by an exponential decay with a correlation time of $\tau_m \approx 3.5$ s [Fig. 2(d), Ref. [13]). If only a single 1 min waveform, such as in Fig. 2, is used to estimate the variance of $X(t)$, the error is large, approximately 35%, since the number of independent samples $n = \tau_{\mathrm{total}}/\tau_m = 17$ is relatively small.

The signal $X(t)$ obtained with periodic spin randomization is shown in Fig. 2(c), where the randomization is achieved by periodically interrupting the cyclic adiabatic frequency sweeps by a burst of $\pi/2$ pulses, as shown in Fig. 1(c). For this example we use the randomization period $\tau_r = 351$ ms, which corresponds to a $\pi/2$-pulse burst every 500th adiabatic inversion. The burst consists of 20 pulses of 2 μs duration with center frequencies uniformly distributed over the same frequency range as the adiabatic sweeps. Judging from the autocorrelation function of the randomized fluctuations, the spins are very effectively scrambled by this protocol [Fig. 2(d)].

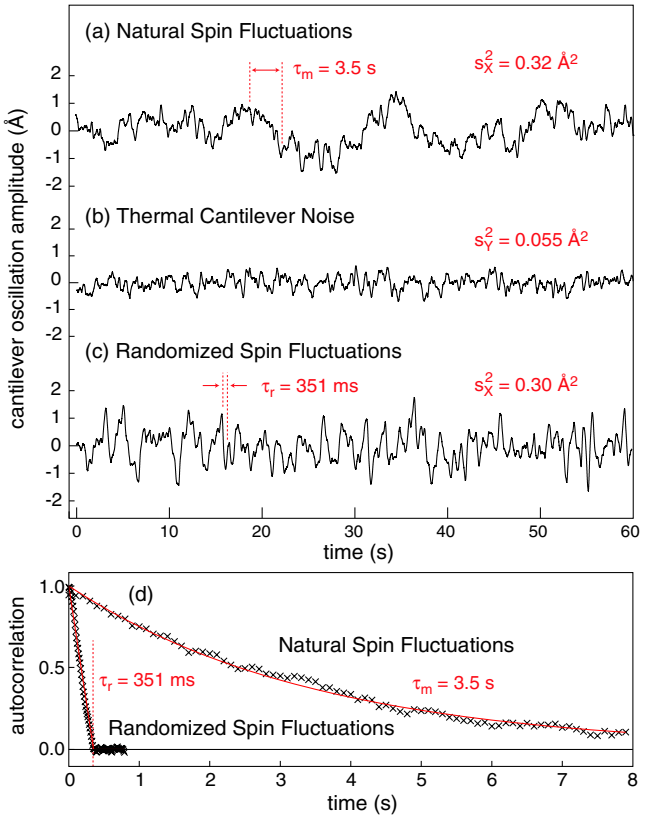

FIG. 2 (color online). Cantilever tip oscillation amplitude as a function of time. (a) In-phase signal $X(t)$ in the presence of the ^{19}F spins fluctuating naturally with a spin signal correlation time of $\tau_m \approx 3.5$ s [13]. (b) Quadrature signal $Y(t)$ due to thermal fluctuations of the cantilever. The observed thermal noise correlation time ($\tau \approx 200$ ms) is set by cantilever and filter bandwidths. (c) Same as (a), but spins are periodically rerandomized every $\tau_r = 351$ ms. (d) Normalized autocorrelation function of spin signals obtained by analysis of an 8 min long record and after subtracting the measurement thermal noise autocorrelation function.

As expected, the autocorrelation function falls linearly and reaches zero at τ_r.

The periodic randomization allows us to make an improved estimate of the spin signal variance. Based on a randomization repetition period $\tau_r = 351$ ms and the same total measurement time of 60 s, the number of independent measurements is now $\tau_{\mathrm{total}}/\tau_r = 171$, which results in an uncertainty in the variance of about 11%, an improvement of more than a factor of 3.

To more concretely illustrate the impact of periodic randomization on the SNR, we show in Fig. 3(a) a one-dimensional lateral imaging scan over the CaF_2 object. Each point represents the estimated spin signal variance from a 1 min data record. Two overall signal maxima are visible that result from the two lobes of the imaging point spread function [15]. For the scan with natural spin randomization, the large uncertainty in the variance results in large scatter in the scan data over regions where the spin

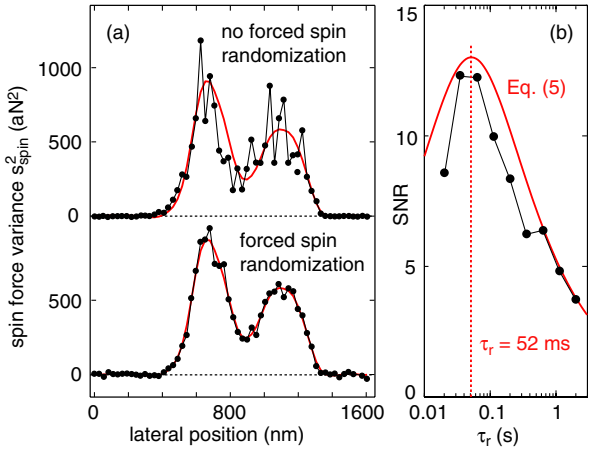

FIG. 3 (color online). (a) One-dimensional image scans in the **x** direction of the calcium fluoride sample. The points are the measured variances of the spin force and the solid lines are guides for the eye. Scatter of the data points in the top image is due to the uncertainty of the variance estimates. Much improved SNR is seen in the lower image where the spins are periodically randomized at $\tau_r = 113$ ms. (b) Data points showing SNR for 1 min measurements as a function of the randomization interval τ_r. The solid line represents the expected SNR based on Eq. (5) using known experimental parameters (no free fit parameters).

signal is highest. The periodic spin randomization, performed with $\tau_r = 113$ ms results in dramatic reduction of the data scatter, especially for the points with the largest spin signal [Fig. 3(a), lower image]. The slightly larger noise in the regions where there is no spin signal is due to increased measurement noise that results from the larger measurement bandwidth needed to accommodate the shortened spin correlation time.

As indicated by Eq. (5) and shown in Fig. 3(b), we can vary τ_r in order to optimize the SNR. Here we measure the spin fluctuations at a position of large spin signal [the 670-nm position of the lateral scan shown in Fig. 3(a)]. To determine each SNR data point, 50 one-minute data records were acquired. The sample variance s^2_{spin} from each record was calculated and the SNR was determined by $\mathrm{SNR} = \overline{s^2_{\mathrm{spin}}}/s_{s^2_{\mathrm{spin}}}$, where $\overline{s^2_{\mathrm{spin}}}$ and $s_{s^2_{\mathrm{spin}}}$ are the mean and the standard deviation of the variances, respectively. As shorter randomization intervals are used, the SNR increases until it reaches a maximum around $\tau_r = 50$ ms. The SNR then drops for the shortest τ_r value tested, as expected, since the large associated measurement bandwidth is admitting more measurement noise than is optimal. Obtaining results for even shorter τ_r was hampered by the finite response time ($\sim$12 ms) of the cantilever.

Figure 3(b) also plots the theoretical SNR according to Eq. (5) using the following parameters determined from the experiment: $\sigma^2_{\mathrm{spin}} = 900$ aN^2 and $S_{\mathrm{noise}} = 66$ aN^2/Hz. The theory predicts an optimal SNR of roughly 13 for a one-minute measurement time when $\tau_r = 52$ ms, in good agreement with the experimental results. Overall, the SNR values obtained experimentally are just slightly lower than predicted by Eq. (5) [14].

In conclusion, we have shown that noise inherent in the measurement of small, statistically polarized spin ensembles can be mitigated by rapid rerandomization of the spins. Beyond the fundamental interest in the control and measurement of spin ensembles in the nanometer regime, the practical impact on nanoscale magnetic resonance imaging is significant: the demonstrated 6× improvement in SNR allows a 36× increase of imaging speed.

We thank C. Rettner, M. Hart, and M. Farinelli for fabrication of the microwire and the magnetic tip, B. W. Chui for cantilever fabrication, and D. Pearson and B. Melior for technical support. We acknowledge support from the DARPA QUIST program administered through the U.S. Army Research Office, and the Stanford-IBM Center for Probing the Nanoscale, a NSF Nanoscale Science and Engineering Center. C. L. D. acknowledges funding from the Swiss National Science Foundation.

*rugar@almaden.ibm.com

[1] J. A. Sidles *et al.*, Rev. Mod. Phys. **67**, 249 (1995).
[2] H. J. Mamin *et al.*, Nature Nanotechnology **2**, 301 (2007).
[3] F. Bloch, Phys. Rev. **70**, 460 (1946).
[4] T. Sleator *et al.*, Phys. Rev. Lett. **55**, 1742 (1985).
[5] M. A. McCoy and R. R. Ernst, Chem. Phys. Lett. **159**, 587 (1989).
[6] M. Guéron and J. L. Leroy, J. Magn. Reson. **85**, 209 (1989).
[7] N. Müller and A. Jerschow, Proc. Natl. Acad. Sci. U.S.A. **103**, 6790 (2006).
[8] S. A. Crooker *et al.*, Nature (London) **431**, 49 (2004).
[9] H. J. Mamin *et al.*, Phys. Rev. B **72**, 024413 (2005).
[10] A. Abragam, *Principles of Nuclear Magnetic Resonance* (Oxford, New York, 1961), p. 133.
[11] E. L. Lehmann, *Theory of Point Estimation* (Wiley, New York, 1983), p. 106.
[12] D. Rugar *et al.*, Science **264**, 1560 (1994).
[13] τ_m is closely related to the intrinsic rotating-frame spin lifetime $T_{1\rho}$ and also depends on a number of extrinsic parameters, for example, the amplitude and modulation of the rf field B_1. See also Slichter, pp. 244–246 (Ref. [17]).
[14] This predicted slight reduction in SNR is in agreement with a more general analysis we have performed that can accommodate all types of filtering. See S. O. Rice, Bell Syst. Tech. J. **24**, 46 (1945); see also R. A. Webb, R. P. Giffard, and J. C. Wheatley, J. Low Temp. Phys. **13**, 383 (1973).
[15] O. Züger, S. T. Hoen, C. S. Yannoni, and D. Rugar, J. Appl. Phys. **79**, 1881 (1996).
[16] M. Poggio, C. L. Degen, H. J. Mamin, and D. Rugar, Appl. Phys. Lett. **90**, 263111 (2007).
[17] C. P. Slichter, *Principles of Magnetic Resonance* (Springer, Berlin, 1990), 3rd ed., pp. 20–24.
[18] L. A. Madsen, G. M. Leskowitz, and D. P. Weitekamp, Proc. Natl. Acad. Sci. U.S.A. **101**, 12804 (2004).